# GEOMETRIC REGISTRATION AND CLASSIFICATION OF HYPERSPECTRAL AIRBORNE PUSHBROOM DATA

**J. S. BETHEL[*], C. LEE[*], D. A. LANDGREBE[**]**
[*]Purdue University
Geomatics Area, School of Civil Engineering
[**]Purdue University
School of Electrical and Computer Engineering

bethel, changno, landgreb@ecn.purdue.edu

Working Group III/5

**KEY WORDS:** Mathematical models, Orientation, Hyperspectral, Image registration, Remote sensing, Multispectral, Classification

## ABSTRACT

Innovative geometric modeling techniques involving stochastic constraints and linear feature exploitation have been demonstrated to yield good results in the rectification of hyperspectral airborne pushbroom imagery. The unique aspects of the platform trajectory are particularly well addressed by these techniques. Supervised statistical pattern recognition techniques have been developed specifically to address the unique and challenging aspects of high dimensional data. These have resulted in processing strategies which are compatible with common desktop computing resources. The combination of such thematic class extraction with effective rectification algorithms delivers a powerful tool into the hands of those building urban databases.

## 1 INTRODUCTION

Hyperspectral data analysis has repeatedly been shown to yield high quality thematic class maps in urban areas. Rigorous geometric sensor and platform modeling have been shown to yield high quality geometric registrations with such imagery. But it has been a rare occurrence for these results to be achieved simultaneously. By using an interdisciplinary approach to this problem, we have developed a set of interdependent algorithms which collectively produce accurate thematic material and region delineations. Other experience has also confirmed that such interdisciplinary data fusion is the way that such analysis should be carried out. Data used for the following analysis was acquired by the HYDICE (Hyperspectral Digital Imagery Collection Experiment) sensor. It is a pushbroom airborne imaging spectrometer with 210 spectral channels ranging from 0.4 to 2.5 micrometers. It has an instantaneous field of view, IFOV, of 0.5 mrad. The ground sample distance, GSD, is generally 2-3 meters. It operates with a gyro stabilized platform referred to as the FSP.

## 2 GEOMETRIC REGISTRATION

The basic principle of the geometry in a pushbroom imaging system can be explained by the collinearity condition, which requires that a light ray from the ground object to the image point should be a straight line. In this case, we need six elements of exterior orientation (EO) for each scan line because the pushbroom image is collected sequentially line by line. Consequently so many parameters may need to be solved for that the problem becomes infeasible due to the number of required control data in most cases. This situation can be addressed by using *a priori* information about the behavior of the platform.

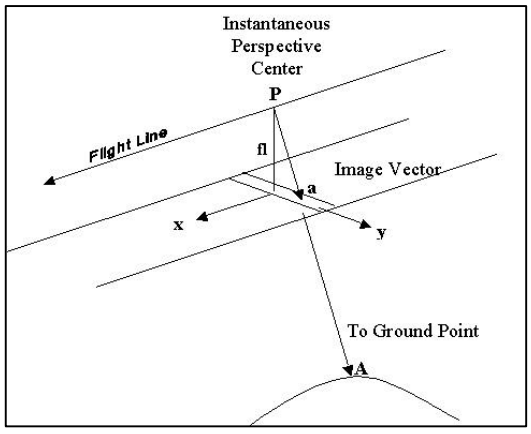


Figure 1 HYDICE imaging system

### 2.1 Collinearity Equations

The geometric relationship between the ground point and image point of HYDICE imagery can be simplified as shown in Figure 1 for a given scan line. From Figure 1, the

collinearity equation can be derived easily as in frame photography. The sensor coordinate system (SCS) is a three-dimensional coordinate system for the image vector in the collinearity equations. The origin of the SCS is determined as the instantaneous perspective center. The x-direction is coincident to line direction ("along track", in the direction of the platform motion) and the y-direction is the same as the column direction ("cross track"). The z-direction can be determined by requiring a right-handed coordinate system. The z-coordinate of the image vector is fixed to -*fl*, where *fl* is the "calibrated" focal length. The calibrated focal length can be considered a constant value over the entire image and needs to be estimated because only a nominal value (79mm) is available. The relationship between the ground coordinates and corresponding image coordinates can then be expressed as equation (1) – (3).

$$F_x = x + fl\frac{U}{W} = 0 \tag{1}$$

$$F_y = y + fl\frac{V}{W} = 0 \tag{2}$$

$$\begin{bmatrix} U \\ V \\ W \end{bmatrix} = M \begin{bmatrix} X - X_L \\ Y - Y_L \\ Z - Z_L \end{bmatrix} \tag{3}$$

where $x, y$ : x, y coordinates of image point in image coordinate system

$X, Y, Z$ : X, Y, Z coordinates of object point in ground coordinate system

$X_L, Y_L, Z_L$ : X, Y, Z coordinates of instantaneous perspective center in ground coordinate system

$M$ : 3×3 orthogonal rotation matrix from the ground coordinate system to image coordinate system

$fl$ : calibrated focal length

From equation (1) – (3), notice that the six EO (Exterior Orientation) parameters, consisting of three coordinates ($X_L, Y_L, Z_L$) of the instantaneous perspective center position, and three independent rotational angles (ω, φ, κ), have different values for each scan line. Therefore, at least three control points are required for each scan line.

This problem can be addressed by using *a priori* information describing the platform behavior. Even though the HYDICE sensor may encounter severe air stream turbulence during its flight, the FSP preserves the sensor optical axis within one degree of nadir when the aircraft pitch and roll angles are within 5 degrees of level flight. Aircraft crew performs aircraft operations to keep the nominal trajectory with a certain range. The time interval between two adjacent lines is very short (8.3 - 50 *msec*). Therefore each of the six exterior parameters may change slowly as the line number increases. Also each EO parameter in a given scan line will be highly correlated to that in a neighboring scan line.

Based on these assumptions, many models have been proposed and subjected to experiment. The spline model has been often used to model platform trajectories in time-dependent imaging applications. This approach involves the recovery of spline coefficients, with time as the independent variable, for each of the six elements of exterior orientation. Since the time interval between exposure of adjacent lines of imagery is constant, as determined by time tags in the data file, the six time-dependent elements of exterior orientation may be written as a function of line number. The spline model, although acceptable for modeling the general trend of an aircraft trajectory, is too rigid and too restrictive of control point distribution to accurately rectify airborne pushbroom imagery. The Gauss-Markov model, which is based on Gauss Markov process, is flexible in the sense that it can accommodate abrupt changes in the position and orientation of the sensor aboard the aircraft.

### 2.2 Gauss Markov Process

The Gauss-Markov (GM) process is a very useful process in engineering applications because many physical processes are well described by its stochastic properties, and because its mathematical description is relatively simple.

The criterion for a first order Markov process is that the conditional probability distribution of a random process be dependent only on the one most recent point in the past. For the first order GM, we can make fictitious observations for 6 EO per each line starting the second line,

$$F_G = e^{-s_p} \cdot (\Delta p)_{i-1} - (\Delta p)_i = 0 \tag{4}$$

where $\Delta p$ is correction of each 6 EO element

$i$ is line number in the image($i$ = 2,3,...,1280)

$s$ is coefficient for each EO element

Similarly, the second order Gauss-Markov process can be defined as a gaussian random process whose conditional probability distribution is dependent only on the two previous points. The related fictitious observation equation is

$$F_G = (a_1)_p \cdot \Delta p_{i-1} + (a_2)_p \cdot \Delta p_{i-2} - \Delta p_i = 0 \quad (5)$$

$$a_1 = \frac{(1+s)\cdot e^{-s}\cdot\left\{1-(1+2s)\cdot e^{-2s}\right\}}{1-(1+s)^2 e^{-2s}} \quad (6)$$

$$a_2 = \frac{-s^2 e^{-2s}}{1-(1+s)^2 e^{-2s}} \quad (7)$$

where $\Delta p$ is correction of each 6 EO element
$i$ is line number in the image($i$ = 3,4,...,1280)
$s$ is coefficient for each EO element

Note that GM process is applied to the corrections of the six EO elements instead of the six elements themselves.
By adding these fictitious observation equations to the conventional observation equations, 6 EO parameters for each image line are tied, or constrained, stochastically to other image lines in close proximity. This model allows for greater flexibility for linear feature constraints to contribute to parameter recovery, thereby improving rectification accuracy.

### 2.3 Exploitation of Ground Line Features

The most common control feature used in the triangulation of multispectral imagery as well as traditional frame photography is the control point. In our data set, the control points coordinates were obtained from triangulated frame photography that included the HYDICE coverage.
Linear features can be defined as the linked edges that determine object boundaries. Although linear features have not been widely used in the estimation of exterior orientation (EO) for the time-dependent sensor, many experiments have been performed and have proven the usefulness of linear features in frame photography applications.
For the pushbroom airborne imaging system, linear features can serve as high-density control data so that high frequency distortion can be detected and corrected. As can be seen from the raw HYDICE images, the linear features which suffer worst from roll-induced displacements occur mainly in the direction of the flight line, while linear features, which are almost perpendicular to the flight line, showed little distortion. Therefore, the linear features in the direction of 'across track' are not helpful to detect high frequency roll-induced distortion.
Although the term linear feature encompasses any continuous feature with a negligible width and includes such parameterizations as splines, we concern ourselves with the special case of straight-line segments in the remainder of the paper.

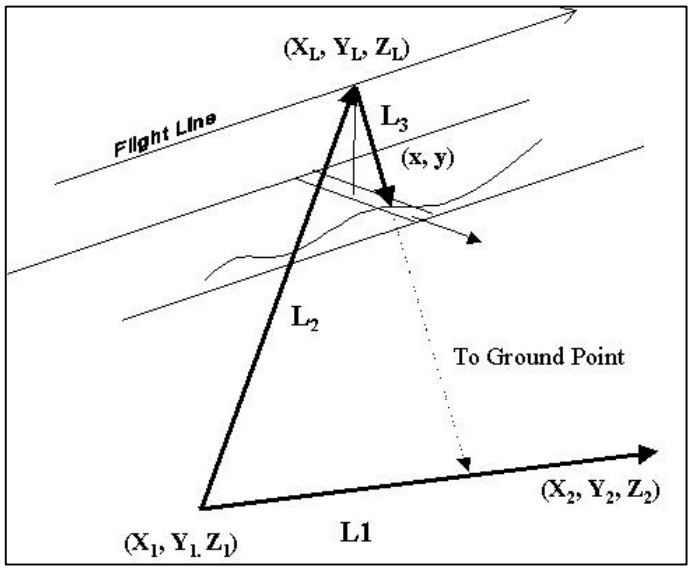


Figure 2 Control Line Model

**2.3.1 Control Line Model.** Line can be used as control data like control point. At a given scan line, a image vector L3, which is rotated to the ground coordinate system, is on a plane that is defined by the three points, two end points of the line on the ground space and the position of instantaneous perspective center. Therefore the determinant of the three vector in figure 2 should be equal to zero. The control line model can be expressed as follows:

$$F_P = |L1 \quad L2 \quad L3| = 0 \quad (8)$$

where

$$L1 = \begin{bmatrix} X_2 - X_1 & Y_2 - Y_1 & Z_2 - Z_1 \end{bmatrix}^T$$

$$L2 = \begin{bmatrix} X_L - X_1 & Y_L - Y_1 & Z_L - Z_1 \end{bmatrix}^T$$

$$L3 = M^T \begin{bmatrix} x & y & -fl \end{bmatrix}^T$$

**2.3.2 Constrained Line Model.** Straight-line features also can be used to constrain point observations on a line. Note that image vectors on a given line are nearly

parallel and vertical. Therefore the elevation of a constrained line couldn't be estimated reliably. To relieve this situation, we need to assume that linear features are horizontal in the ground space with known elevation. Then the constrained line model can be made based on the fact that three consecutive points should be on a straight line in the ground space.

$$F_P = \begin{vmatrix} 1 & 1 & 1 \\ X_1 & X_2 & X_3 \\ Y_1 & Y_2 & Y_3 \end{vmatrix} = 0 \tag{9}$$

$$X_i = (Z_i - Z_L)\frac{U_t}{W_t}$$

$$Y_i = (Z_i - Z_L)\frac{V_t}{W_t}$$

where $$\begin{bmatrix} U_t & V_t & W_t \end{bmatrix}^T = M^T \begin{bmatrix} x_i & y_i & -fl \end{bmatrix}$$

**2.3.3 Semi-automated Line Extraction.** As mentioned previously, the sampling rate is an important factor for the Gauss-Markov model. To increase the sampling rate, it is desirable to extract each point on every scan line for each linear feature. Digitizing points manually on the line is time consuming and error-prone work. Fortunately, this time consuming work can be replaced by a semi-automatic method, which extracts lines automatically given initial approximate delineation. The method used in this paper is based on time-delayed discrete dynamic programming for energy minimization of active contours [Amini, et. al., 1990]. In this method, we start with an initial line that is determined approximately. The position of the line is updated by the influence of image gradients near the edge, and by internal smoothness of the line. The update continues until no change is produced in the estimated line position.
An energy minimization model has been often used to extract linear features. A typical objective function of such an energy minimizing model can be expressed by equation (10).

$$Min. \quad E = \sum_{i=1}^{n} \left[ E_{\text{int}}(p_i) + E_{\text{edge}}(p_i) \right] \tag{10}$$

where, $$E_{\text{int}}(p_i) = \left( \alpha \left| p_i - p_{i-1} \right|^2 + \beta \left| p_{i+1} - 2p_i + p_{i-1} \right|^2 \right) \tag{11}$$

$E_{\text{edge}}(p_i)$ : Energy function related to image gradient

$p_i$ : position $(l,c)$ of $i^{th}$ point on the line

$\alpha$, $\beta$: coefficients

This function consists of two energy functions, internal energy and edge energy. The internal energy serves as the forces that make the line to be smooth. The first term of internal energy is used to make consecutive points closer to one another and the second term makes the shape of line smooth. The edge energy represents the forces that make the line take the shape of salient features present in the image. Thus, the line is attracted to image points with high gradient values.
Dynamic programming is a very useful method for the solution of many optimization problems where a sequence of inter-related decisions is required. For many optimization problems, it is often possible to decompose a problem into a sequence of smaller sub-problems. Then, these problems can be solved recursively one at a time. Therefore, computational effort can be reduced significantly.

## 2.4 Experiments

The purpose of this section is to compare the accuracy obtained from the restitution of HYDICE imagery using different platform models. In order to quantify the performance of each model, we examine the residuals of check points. Since we have only single image coverage, the Z-coordinate must be fixed to its known value. This does not imply a flat terrain assumption, only that the various Z coordinates of points and features are indeterminate using a single image. The estimated coordinates, $X_{est}$ and $Y_{est}$, are computed as follows:

$$X_{est} = (Z - Z_L)\frac{U_t}{W_t} + X_L \tag{12}$$

$$Y_{est} = (Z - Z_L)\frac{V_t}{W_t} + Y_L \tag{13}$$

where $\begin{bmatrix} U_t & V_t & W_t \end{bmatrix}^T = M^T \begin{bmatrix} x & y & -fl \end{bmatrix}^T$

From equation (12), $Z$ is a known coordinate of the check point. The residuals are then the differences between the estimated and known values.

$$X_{res} = X_{est} - X \tag{14}$$

$$Y_{res} = Y_{est} - Y \tag{15}$$

where $X, Y$ are the known check point ground coordinates

**2.4.1 Contribution of Control Lines.** Experiments were run to test the contribution of linear features with the first and second order Gauss-Markov model for varying control features. First, only control points were used to determine the unknown parameters. Next, the experiments were repeated with control lines in addition to control points. For the first order Gauss-Markov model, two data sets showed similar results. Adding straight line features to the solution improves ΔY (cross track) of check points and check lines significantly, while ΔX (along track) of check points were essentially same: see Tables 1. The second order Gauss-Markov model showed similar results except ΔX of the check points for the Washington, DC data set (Tables 1). Adding control lines reduced the RMS residual ΔX of check points of the Washington, DC data set significantly. The results from the first order GM model slightly better than those from the second order GM model.

Table 1 Contribution of Control Lines

| GM | Control Data | Check Point RMS (m); Washington, DC | | | Check Point RMS (m); Fort Hood | | |
|---|---|---|---|---|---|---|---|
| | | ΔX | ΔY | Δd | ΔX | ΔY | Δd |
| First order | Point only | 1.95 | 1.99 | 2.79 | 1.61 | 2.30 | 2.81 |
| | Point and Line | 1.98 | 1.61 | 2.55 | 1.50 | 1.32 | 2.00 |
| Second order | Point only | 2.50 | 2.14 | 3.29 | 1.67 | 1.53 | 2.26 |
| | Point and Line | 2.01 | 1.59 | 2.56 | 1.61 | 1.25 | 2.04 |

**2.4.2 Comparison of Line Models.** Two different line models were tested and compared in table 2. The results of the control line model is significantly better than those of the constrained line model for the RMS residual ΔY with both of data sets, while the difference of ΔX of check points was insignificant.

Table 2 Comparison of Line Models

| Line Model | Check Point RMS (m); Washington, DC | | | Check Point RMS (m); Fort Hood | | |
|---|---|---|---|---|---|---|
| | ΔX | ΔY | Δd | ΔX | ΔY | Δd |
| Control Line | 1.98 | 1.61 | 2.55 | 1.50 | 1.32 | 2.00 |
| Constrained Line | 1.93 | 2.02 | 2.79 | 1.64 | 1.74 | 2.39 |

## 3 EXTRACTION OF THEMATIC CLASSES BY MULTISPECTRAL ANALYSIS

Hyperspectral image data such as that produced by the HYDICE sensor system provide a rich source of spectral information in image form that can be easily exploited in the task of generating a thematic map of an area. The more than 200 samples of the spectrum of reflected energy provide ample detail of the spectral response reflected from a

complex surface such as that of the Earth. However, such data also present some significant subtleties that must be well understood and properly dealt with if the full information-bearing potential of such data is to be realized.

Any given material on the Earth's surface that one may wish to map will exist in a number of states. This leads to a given material being characterized by not a single spectral response but by a family or ensemble of spectral responses. Quite in addition to a typical or average response, the more general ensemble properties will have characteristics useful for purposes of discriminating between materials in that scene. For example, pixels measured of an agricultural crop on a given day vary somewhat and this variation will be significantly diagnostic of that crop. Even though the leaves of the crop may have spectral characteristics very similar to those of a tree species, a pixel that includes a number of crop plants will carry with it characteristics unique to the crop and different from those of a wooded area, because of the difference in physical structure of the two types of plants.
Thus, the process of mapping themes of the Earth's surface is one of labeling pixels whose ensemble have variations that are characteristic of the themes of interest. One is not looking simply for the similarity of a pixel to some spectral standard so much as looking at the similarity or difference of mixtures of pixel responses.

The most effective way to represent data for this purpose is in terms of a feature space. The concept is to represent the data values of each pixel as components of a vector. Thus a pixel of 200 band data would be a point in a 200 dimensional vector space, and an ensemble of pixels that represent a given class of surface cover would be a distribution in this 200 dimensional vector space.

The power of hyperspectral data can then be simply illustrated by noting that if one has data measured in 200 bands each with 10 bit precision ($2^{10}$ = 1024 shades of gray), then there are $2^{10}$ raised to the $200^{th}$ power individual locations in that feature space for a pixel to be found. That number, $2^{2000} \sim 10^{600}$ is so large that even if one has a data set of a million pixels, the probability of any two pixels occurring in the same location in this space is vanishingly small. Thus, since there is no overlap, theoretically, anything is separable from anything else. The difficulty, on the other hand, is that one must locate decision boundaries between desired classes in such a large space very precisely in order to achieve successful discrimination between all the classes existing in such a data set. That is the task that the analyst faces.

Much has been learned in the last few years about how to accomplish this analysis.[1] An important example of this stems from the fact that, because of the large volume of hyperspectral feature spaces, most of the volume available for a given data set will be empty, and the significant structure for a specific problem at hand will reside in a lower dimensional subspace. Thus it is useful to define an optimal linear transformation on the specific data classes desired to find the lower dimensional space most useful for discriminating the data into desired classes. Such transformations are known as feature extraction algorithms.

A group of algorithms for accomplishing the this and other necessary processes have been assembled and made available to the public in a program for personal computers called MultiSpec.[2] Though there are a number of details and variations, the basic analysis process is one of

1. Defining the classes of interest to the analyst by labeling an adequate number of examples of each in the data set itself.
2. Exercising a feature extraction algorithm that basically defines an optimal subspace for this particular classification.
3. Choosing and executing an appropriate classification algorithm in the chosen subspace.

The process has become simple enough that a sizable hyperspectral data set of perhaps 150 megabytes can be analyzed to create a thematic map for 6 to 10 user themes in less than half an hour using less than 3 minutes of computation time on a contemporary $3000 personal computer.

Figure 3 shows an image sequence of such an analysis of a HYDICE data set of the Washington, DC mall area. The data set contains 1208 scan lines of 307 pixels (˜370,000 pixels) in 210 bands. The primary task of the analyst is to specify what classes of surface cover one wishes to discriminate between. In this case, the desired user classes were Roofs, Road, Grass, Trees, Water and an additional class called Trail to account for the gravel pathways down the mall itself. An additional class called Shadow was also added to account for the fact that shadow areas will be spectrally

[1] See for example, David Landgrebe, "Information Extraction Principles and Methods for Multispectral and Hyperspectral Image Data," Chapter 1 of *Information Processing for Remote Sensing,* edited by C. H. Chen, published by the World Scientific Publishing Co., Inc., 1060 Main Street, River Edge, NJ 07661, USA 1999. This chapter is also available for download at
http://dynamo.ecn.purdue.edu/~landgreb/publications.html.

[2] MultiSpec and its documentation is available for download at
http://dynamo.ecn.purdue.edu/~biehl/MultiSpec/

different from directly illuminated areas; because they are quite dark, they would not be that different spectrally from water in the scene. It is a fundamental requirement that the list of classes must be reasonably exhaustive.

To illustrate the role that the human analyst must play in the process, note that some rooftops are made of gravel/asphalt mixtures, the same materials used in some roads. In this case it is desired to discriminate between these two classes of use, and it would be necessary for the analyst to label examples of each if a classifier is to successfully discriminate between them.

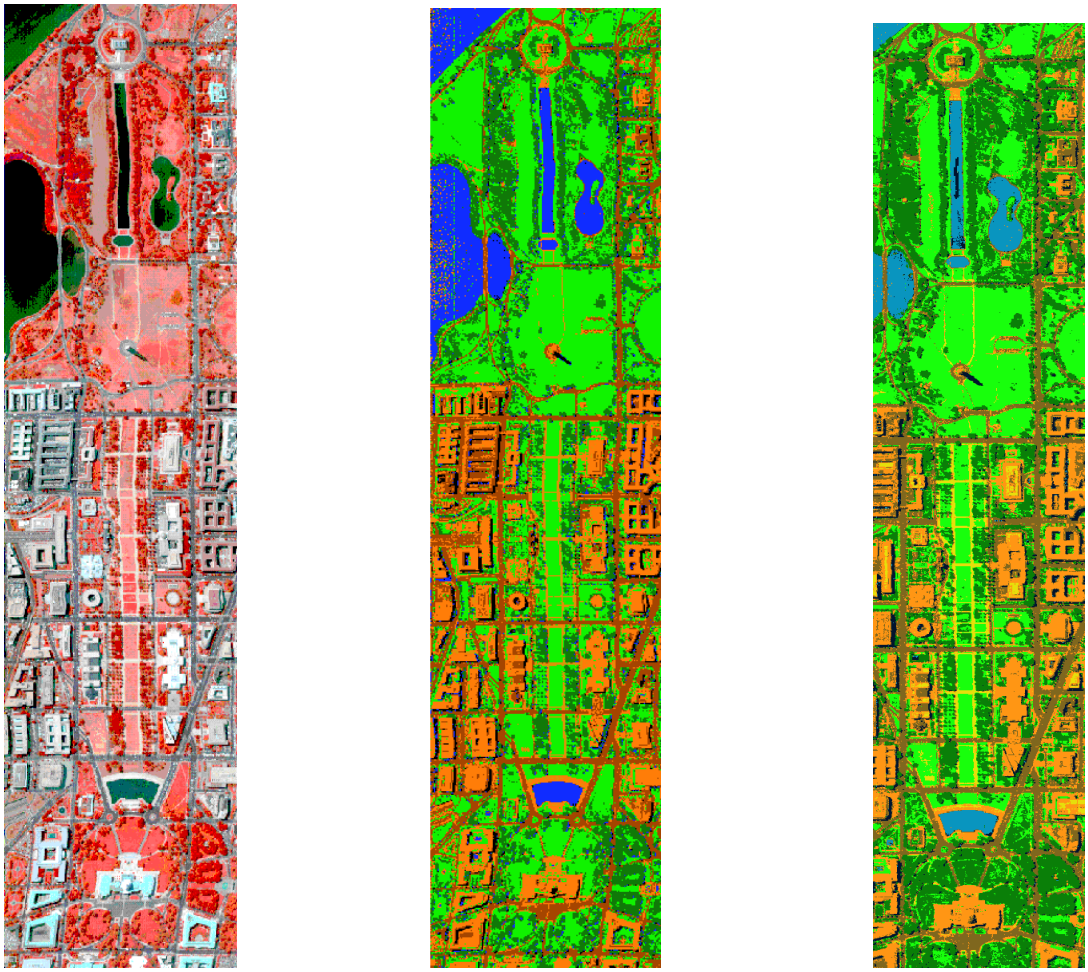

Figure 3 Image Sequence: Raw Image, Thematic Classes, Rectified Thematic Classes


Figure 4. Class labels for the Thematic Image

## 4 CONCLUSIONS

The increased spectral resolution afforded by hyperspectral sensors such as HYDICE, together with appropriately designed statistical pattern recognition algorithms, can yield excellent and reliable material and land cover region delineation. Proper modeling of the atmospheric turbulence driven variability in the host aircraft position and angular trajectory can yield accurate transformations between image and ground coordinates. The combination of these two approaches to image exploitation, which have traditionally been carried out in isolation, provides unique information toward the rigorous development of 3D databases in which the features and textures are both correctly labeled and correctly positioned.

## ACKNOWLEDGMENTS

The work described in this paper was sponsored by the U.S. Army Research Office under Grant Number DAAH04-96-1-0444. The authors would like to acknowledge the support of Dr. Edward Mikhail, the project director. They would also like to thank Hank Theiss for his help in data analysis.

## REFERENCES

1. Amini, A., Weymouth, T., Jain, R., "Using dynamic programming for solving variational problems in vision", IEEE Transactions on Pattern Analysis and machine Intelligence, Vol. 12, No. 9, 1990.
2. Landgrebe, D., 1999, "Information Extraction Principles and Methods for Multispectral and Hyperspectral Image Data", Chapter 1 of *Information Processing for Remote Sensing*, edited by C.H. Chen, World Scientific Publishing Co., River Edge, NJ
3. Lee, C., Theiss, H., Bethel, J., Mikhail, E., 2000, "Rigorous Mathematical Modeling of Airborne Pushbroom Imaging Systems", Photogrammetric Engineering and Remote Sensing, Vol. 66, No. 4, April 2000, pp. 385-392.
4. Mikhail, E., and McGlone, C., 1980, "Current Status of Metric Reduction of (Passive) Scanner Data", Proceedings of ISPRS Congress, Commission III, WG III-1, p.504. Hamburg